Journal of Applied Fluid Mechanics, Vol. 9, No. 5, pp. 2217-2227, 2016.
Available online at www.jafmonline.net, ISSN 1735-3572, EISSN 1735-3645.
DOI: 10.18869/acadpub.jafm.68.236.25513

Theoretical Analysis of Shear Thinning Hyperbolic Tangent Fluid Model for Blood Flow in Curved Artery with Stenosis

S. Nadeem† and S. Ijaz

Department of Mathematics, Quaid-i-Azam University 45320 *, Islamabad* 44000 *Pakistan*

†Corresponding Author Email:Shagufta.me2011@yahoo.com

(Received August, 18, 2015; accepted December 28, 2015)

ABSTRACT

In this paper, we have considered the blood flow in a curved channel with abnormal development of stenosis in an axis-symmetric manner. The constitutive equations for incompressible and steady non-Newtonian tangent hyperbolic fluid have been modeled under the mild stenosis case. A perturbation technique and homotopy perturbation technique have been used to obtain analytical solutions for the wall shear stress, resistance impedance to flow, wall shear stress at the stenosis throat and velocity profile. The obtained results have been discussed for different tapered arteries i.e., diverging tapering, converging tapering, non-tapered arteries with the help of different parameters of interest and found that tapering dominant the curvature of the curved channel.

Keywords: Curved artery; Blood flow; Stenosis; Analytical solutions; Hyperbolic tangent fluid model.

NOMENCLATURE

a	indicate stenosis position	U, V	components of velocity
b	length of stenosis	w_e	Weissenberg number
C_i	constants (i=1-10)	x	axial direction
e_0	radius of normal artery		
F	flow rate	ε	tapering parameter
$h(x)$	height of stenosis	$\bar{\dot{\gamma}}_0$	extra stress tensor
L	length of stenosed artery	δ	maximum height of stenosis
$n \geq 2$	stenosis shape	λ	resistance impedance
n_e	fluid parameter	λ_0	resistance (no stenosis)
P	pressure	μ_∞	shear rate viscosity at infinity
Q	embedding parameter	μ_0	shear rate viscosity at zero
R_{en}	Reynolds number	τ_o	shear stress (no stenosis)
r	radial direction	Π	second invariant strain tensor
R_c	curvature	$\bar{\dot{\gamma}}$	shear rate
S_{rr}, S_{rx}, S_{xx}	shear stress	Γ	time constant
u_o	averaged velocity	φ	tapering parameter
$(-,*)$	denotes the non-dimensional quantities	$\eta, \sigma, \zeta, \varepsilon, a_j$ (j=1-4)	constants

1. INTRODUCTION

Most of the cardiovascular diseases, especially atherosclerosis or stenosis have been found to be responsible for major deaths in both developing and developed countries. It occurs to deposition of proliferation in the connective tissues and cholesterol in the arterial wall. The presence of stenosis at one or more major location may lead to disorders in circulatory systems and different arterial diseases such as myocardial, angina pectoris, coronary thrombosis, infarction and strokes etc. Young *et al*. (1973) investigated axisymmetric and nonsymmetric plastic models. Hassan *et al*. (2008) investigated the laminar sinusoidal pulsating flow through a modeled arterial stenosis with a trapezoidal profile. Mandal *et al*. (2010) investigated numerical solutions of the steady viscous flow due to arterial disease through different double stenosed artery. Nadeem *et al.* (2015) investigated the viscous fluid model through an axis-symmetric stenosis with the effect of three different types of arteries.

The rheological study of blood flow has several goals such as not only to understanding health and disease issues but also that what kind of fluid it is in nature. Some researchers considered blood as a Newtonian fluid especially flows of blood in the large vessels such as the aorta. Liu *et al*. (2004) investigated the pulsating blood flow through models of stenotic and tapered arteries to discuss the distributions of the wall shear stress. In fact blood flow through constricted arteries behaves like a non-Newtonian fluid at low shear rates being suspension of plasma, white cells, red cells and platelets. Canic *et al*. (2003) investigated the quasilinear effects arising in a hyperbolic system of partial differential equations modelling blood flow through large compliant. Sankar *et al*. (2004) discussed the effects of catheterization and non-Newtonian nature of blood in small arteries mathematically by modeling blood as a Herschel-Bulkley fluid. Mekheimer and ElKot *(*2008) discussed the micropolar fluid model for axis-symmetric blood flow through radially symmetric but axially nonsymmetric mild stenosis tapered arteries. Sankar *et al*. (2009) discussed the mathematical model of pulsatile flow of non-Newtonian fluid in stenosed arteries. Here they discussed the Herschel Bulkley fluid and found an analytical solution by using a regular perturbation method. Nadeem *et al*. (2012) investigated the blood flow through a tapered artery with a stenosis assuming the flow is steady and treated blood as hyperbolic tangent fluid. Reddy *et al*. (2014) investigated the blood flow between the clogged (stenotic) artery and the catheter with asymmetric nature of the stenosis. Jung *et al*. (2014) investigated the hemodynamics behavior of the blood flow in the presence of the arterial stenosis. Ellahi *et al*. (2014) discussed the blood flow model through composite stenosis. Here they treated blood as a micropolar fluid model under the mild stenosis case. Nadeem *et al*. (2009 and 2015) investigated the two-dimensional equations of tangent hyperbolic fluid using the assumptions of low Reynolds number and long wavelength

In all the studies that are cited above, the arteries carrying blood were considered to being horizontal. It is widely known that many vessels in physiological systems are not the horizontal because some have the inclination and some are the curve. Chakraborty *et al*. (2011) discussed the suspension model of blood flow through an inclined tube by considering an axially non-symmetric stenosis. However no work has done yet for blood flow in a curved artery (channel) with stenosis but some work has done for peristalsis. Nadeem *et al*. (2013) discussed the peristaltic flow of the tangent hyperbolic fluid in a curved symmetric channel with sinusoidal waves.

Motivated by the above analysis we have considered bloodflow in curved arteries having mild stenosis and treated blood as non-Newtonian tangent hyperbolic fluid. The governing equations for a tangent hyperbolic fluid in a curved artery (or curved channel) along with the effects of curvature are modeled and solved analytically with the help of regular perturbation method and homotopy perturbation method. The comparison of both analytical methods shows that the solutions are almost same for small physical parameters. In the end physical phenomena of the present analysis have been discussed by plotting the graph of wall shear stress, resistance impedance to flow by numerical integration, velocity profile and stream lines.

2. FORMULATION OF THE PROBLEM

We consider the flow of an incompressible non-Newtonian tangent hyperbolic fluid in a curved artery of radius R^* with center O, components of velocity in radial r and axial x directions are $\overline{V}$ and $\overline{U}$ respectively. The equations for conservation of mass and momentum can be written as,

$$\frac{\partial}{\partial \overline{r}}\left(\left(\overline{r}+R^*\right)\overline{V}\right)+R^*\frac{\partial \overline{U}}{\partial \overline{x}}=0, \tag{1}$$

$$\rho\left(\overline{V}\frac{\partial \overline{V}}{\partial \overline{r}}+\frac{R^*}{\overline{r}+R^*}\frac{\partial \overline{V}}{\partial \overline{x}}-\frac{\overline{U}^2}{\overline{r}+R^*}\right)=$$
$$-\frac{\partial \overline{P}}{\partial \overline{r}}+\frac{1}{\overline{r}+R^*}\frac{\partial}{\partial \overline{r}}\left(\left(\overline{r}+R^*\right)\overline{S}_{\overline{r}\overline{r}}\right)$$
$$+\frac{R^*}{\overline{r}+R^*}\frac{\partial}{\partial \overline{x}}\left(\overline{S}_{\overline{r}\overline{x}}\right)-\frac{\overline{S}_{\overline{x}\overline{x}}}{\overline{r}+R^*}, \tag{2}$$

$$\rho\left(\overline{V}\frac{\partial \overline{U}}{\partial \overline{r}}+\frac{R^*\overline{U}}{\overline{r}+R^*}\frac{\partial \overline{U}}{\partial \overline{x}}+\frac{\overline{U}\overline{V}}{\overline{r}+R^*}\right)=$$
$$-\frac{R^*}{\overline{r}+R^*}\frac{\partial \overline{P}}{\partial \overline{x}}+\frac{1}{(\overline{r}+R^*)^2}$$
$$\left(\frac{\partial}{\partial \overline{r}}(\overline{r}+R^*)^2\overline{S}_{\overline{r}\overline{x}}\right)+\frac{R^*}{\overline{r}+R^*}\frac{\partial}{\partial \overline{x}}\left(\overline{S}_{\overline{x}\overline{x}}\right), \tag{3}$$

Where the constitutive equation for hyperbolic tangent fluid is given by Nadeem *et al*. (2009, 2013, 2015)

$$\overline{\boldsymbol{\tau}}=-\overline{P}\mathbf{I}+\overline{\mathbf{S}}, \tag{4}$$

$$\overline{\mathbf{S}}=[\mu_0+(\mu_\infty+\mu_0)\tanh(\Gamma\bar{\dot{\gamma}})^{n_e}]\bar{\dot{\gamma}}_0, \tag{5}$$

In above equations $\overline{P}$ is defined as pressure, μ_∞ as shear rate viscosity at infinity, μ_0 as shear rate viscosity at zero, Γ as time constant, n_e as power law index and $\bar{\dot{\gamma}}$ as shear rate,

$$\bar{\dot{\gamma}} = \sqrt{\frac{1}{2}\sum_i\sum_j \bar{\dot{\gamma}}_{ij}\,\bar{\dot{\gamma}}_{ji}} = \sqrt{\frac{1}{2}\Pi}, \tag{6}$$

Where $\Pi = tr(\text{grad}(\overline{V}) + \text{grad}(\overline{V})^T)^2$, which is defined as second invariant strain tensor. Now for the cases $\Gamma\bar{\dot{\gamma}} \prec\prec 1$ and $\mu_\infty = 0$, Eq. (5) is reduced to Eq. (7) *as*,

$$\begin{aligned}\overline{\mathbf{S}} &= [\mu_0(\Gamma\dot{\gamma})^{n_e}]\bar{\dot{\gamma}}_0,\\ &= [\mu_0(1-1+\Gamma\bar{\dot{\gamma}})^{n_e}]\bar{\dot{\gamma}}_0 = \mu_0[1+n_e(\Gamma\bar{\dot{\gamma}}-1)]\bar{\dot{\gamma}}_0.\end{aligned} \tag{7}$$

Where $\bar{\dot{\gamma}}_0 = L + L^t$ and extra stress tensor for hyperbolic tangent fluid can written as

$$\begin{aligned}\overline{S}_{\overline{rr}} &= 2\mu_0[1+n_e(\Gamma\bar{\dot{\gamma}}-1)]\frac{\partial\overline{V}}{\partial\overline{r}},\\ \overline{S}_{\overline{rx}} &= \overline{S}_{\overline{rx}} = \mu_0[1+n_e(\Gamma\bar{\dot{\gamma}}-1)]\\ &\left(\frac{\partial\overline{U}}{\partial\overline{r}} + \frac{R^*}{\overline{r}+R^*}\frac{\partial\overline{V}}{\partial\overline{x}} - \frac{\overline{U}}{\overline{r}+R^*}\right),\\ \overline{S}_{\overline{xx}} &= 2\mu_0[1+n_e(\Gamma\bar{\dot{\gamma}}-1)]\left(\frac{R^*}{\overline{r}+R^*}\frac{\partial\overline{U}}{\partial\overline{x}} + \frac{\overline{V}}{\overline{r}+R^*}\right),\end{aligned} \tag{8}$$

The geometry of axis-symmetricstenosis in dimensional form is defined as

$$\begin{aligned}\overline{h}(x) &= e(x)[1-\eta^*(b^{n-1}(\overline{x}-a)-(\overline{x}-a)^n)],\\ &a \le \overline{x} \le a+b,\\ &= e(x),\ \text{or else}\end{aligned} \tag{9}$$

with

$$e(x) = e_0 + \varepsilon\overline{x}, \tag{10}$$

where, in above $e(x)$ is the radius of stenotic arterial segment, e_0 is the radius of a non-stenotic arterial segment, ε is tapering parameter, b is the length of stenosis, where a indicates its position and $n \ge 2$ determine the shape of stenosis. The parameter η^* is given as

$$\eta^* = \frac{\delta^* n^{\frac{n}{n-1}}}{e_0 b^n (n-1)}, \tag{11}$$

where δ is the maximum height of stenosis which is located at

$$\overline{x} = a + \frac{b}{n^{\frac{1}{n-1}}}. \tag{12}$$

Introducing the following non dimensional variables,

$$\begin{aligned}&r = \frac{\overline{r}}{e_0},\ x = \frac{\overline{x}}{b},\ U = \frac{\overline{U}}{u_o},\ V = \frac{b\overline{V}}{u_o\delta},\ P = \frac{e_0^2\overline{P}}{u_o b\mu},\\ &w_e = \frac{\Gamma u_o}{e_0}, R_{en} = \frac{bu_o\rho}{\mu},\ S_{rr} = \frac{b\overline{S}_{\overline{rr}}}{u_o\mu},\\ &\overline{S}_{rx} = \frac{e_0\overline{S}_{\overline{rx}}}{u_o\mu},\\ &S_{xx} = \frac{b\overline{S}_{\overline{xx}}}{u_o\mu},\ \dot{\gamma} = \frac{\bar{\dot{\gamma}}e_o}{u_0}.\end{aligned} \tag{13}$$

Using Eq. (13) mild stenosis case $\delta^* = \frac{\delta}{e_0} \prec\prec 1$ and taking the extra conditions $(\varepsilon = \frac{e_0 n^{(\frac{1}{n-1})}}{b} \approx O(1), R_{en}\frac{\delta n^{(\frac{1}{n-1})}}{b} \prec\prec 1)$, above Eqs. (2), (3) and (8)can be written as

$$\frac{\partial P}{\partial r} = 0, \tag{14}$$

$$-\frac{R_c}{r+R_c}\frac{\partial P}{\partial x} + \frac{1}{(r+R_c)^2}\frac{\partial}{\partial r}\left((r+R_c)^2\,\overline{S}_{rx}\right) = 0, \tag{15}$$

also,

$$\overline{S}_{rx} = (1-n_e)\left(\frac{\partial U}{\partial r} - \frac{U}{r+R_c}\right) + w_e n_e\left(\frac{\partial U}{\partial r} - \frac{U}{r+R_c}\right)^2. \tag{16}$$

Substituting Eq. (16) into Eq. (15) , we arrive at

$$\begin{aligned}&\frac{R_c(r+R_c)}{1-n_e}\frac{\partial P}{\partial x} = (r+R_c)^2\frac{\partial^2 U}{\partial r^2}.\\ &+(r+R_c)\frac{\partial U}{\partial r} - U + \frac{2w_e n_e}{1-n_e}\\ &\left\{(r+R_c)^2\left(\frac{\partial U}{\partial r}\right)\left(\frac{\partial^2 U}{\partial r^2}\right) - (r+R_c)\left(\frac{\partial^2 U}{\partial r^2}\right)U\right\}\end{aligned} \tag{17}$$

The dimensionless boundary conditions are defined as

$$\frac{\partial U}{\partial r} = 0\ \ at\ \ r = 0,\ \ U = 0\ \ at\ \ r = h. \tag{18}$$

The geometry of stenosis in dimensionless form is defined as

$$\begin{aligned}h(x) &= (1+\zeta x)[1-\eta((x-\sigma)-(x-\sigma)^n)]\\ &\sigma \le x \le \sigma+1,\end{aligned} \tag{19}$$

where

$$\begin{aligned}&\eta = \frac{\delta n^{\frac{n}{n-1}}}{(n-1)},\ \delta = \frac{\delta^*}{e_0},\ \sigma = \frac{a}{b},\\ &R_c = \frac{R^*}{e_0},\ \zeta = \frac{\zeta' b}{e_0},\ \zeta = \tan\varphi.\end{aligned} \tag{20}$$

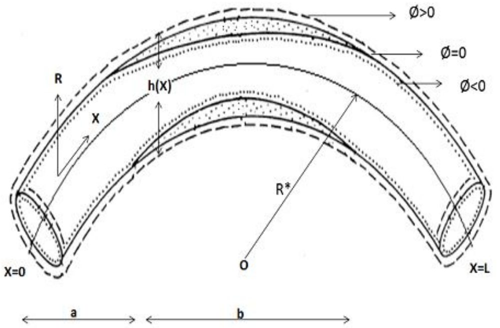

Fig. 1. Geometry of curved arery with

3. SOLUTION OF THE PROBLEM

3.1 Regular Perturbation Solution

According to method we may expand velocity and flow rate by considering w_e as a small parameter

$$U = U_0 + w_e U_1 + w_e^2 U_2 + ...,$$
$$F = F_0 + w_e F_1 + w_e^2 F_2 + ..., \tag{21}$$

With the help of Eq. (21) the solution of Eq. (17) subject to boundary condition (18)takes the following form

$$\begin{aligned} U &= \frac{R_c\left(r+R_c\right)}{1-n_e}\frac{dP}{dx}\left(r+R_c\right)\ln\left(r+R_c\right) = \\ &+\left(C_1+w_eC_3\right)\left(r+R_c\right)+\frac{1}{r+R_c}\left(C_2+w_eC_4\right) \\ &+\frac{a_2w_e}{8\left(r+R_c\right)^3}+\frac{a_3w_e}{2}\left(r+R_c\right)\ln\left(r+R_c\right) \end{aligned} \tag{22}$$

We have defined flow rate as

$$F = \int_0^h U dr, \tag{23}$$

Substituting in Eq. (22) into Eq. (23)weget pressure gradient as follow

$$\frac{dP}{dx} = \frac{F - w_e C_6}{C_5}. \tag{24}$$

Pressure drop ($\Delta P = P$ at $x = 0$ and $\Delta P = -P$ and $x = L$) through the stenosis between the region $x = 0$ and $x = L$ computed from above Eq. (24) can be written as,

$$\Delta P = \int_0^L \left(-\frac{dP}{dx}\right)dx. \tag{25}$$

4. IMPEDANCE RESISTANCE

Using Eq. (25), the resistance can be defined as

$$\begin{aligned} \bar{\lambda} = \frac{\Delta P}{F} &= \{\int_0^a K(x)\,|_{h=1}\,dx + \int_a^{a+b} K(x)dx \\ &+ \int_{a+b}^{L} K(x)\,|_{h=1}\,dx\}, \end{aligned} \tag{26}$$

where

$$K(x) = -\frac{F - w_e C_6}{C_5 F}, \tag{27}$$

Using Eq. (27) into Eq. (26), takes the form

$$\bar{\lambda} = \left(-\frac{F - w_e C_6}{C_5 F}\Bigg|_{h=1}\right)\left(L - b\right) + \int_a^{a+b} K(x)dx. \tag{28}$$

5. WALL SHEAR STRESS EXPRESSIONS

After using dimensionless variables wall shear stress can be defined as

$$\begin{aligned} \bar{S}_{rx} &= [\left(1-n_e\right)\left(\frac{\partial U}{\partial r} - \frac{U}{r+R_c}\right) \\ &+ w_e n_e\left(\frac{\partial U}{\partial r} - \frac{U}{r+R_c}\right)^2]\,|_{r=h}, \end{aligned} \tag{29}$$

The maximum shear stress at the throat of stenosis is located at $x = \frac{a}{b} + \frac{1}{n^{\frac{1}{n-1}}}$ and given as©

$$\bar{\tau}_{rx} = \bar{S}_{rx}\,|_{h=1-\delta}, \tag{30}$$

Finally the expression for λ and S_{rx} can be defined as follows:

$$\bar{S}_{rx} = [\left(1-n_e\right)\left(\frac{\partial U}{\partial r} - \frac{U}{r+R_c}\right) + w_e n_e\left(\frac{\partial U}{\partial r} - \frac{U}{r+R_c}\right)^2]\,|_{r=h}, \tag{31}$$

$$\lambda = \{\left(1-\frac{b}{L}\right)\left(-\frac{F - w_e C_6}{C_5 F}\right)|_{h=1} + \frac{1}{L}\int_a^{a+b} K(x)dx\}, \tag{32}$$

in which

$$\lambda = \frac{\bar{\lambda}}{\lambda_o},\; S_{rx} = \frac{\bar{S}_{rx}}{\tau_o},\; \tau_{rx} = \frac{\bar{\tau}_{rx}}{\tau_o},\; \lambda_o = L,\; \tau_o = F. \tag{33}$$

6. HOMOTOPY PERTURBATION SOLUTIONS

In this section solution have been computed by using homotopy perturbation method suggested by He in (2005), we can write Eq. (17)in operator form

$$0 = L_U + \frac{2w_e n_e}{1-n_e}$$

$$\left[\left(r+R_c\right)^2\left(\frac{\partial U}{\partial r}\right)\left(\frac{\partial^2 U}{\partial r^2}\right)-\left(r+R_c\right)\left(\frac{\partial^2 U}{\partial r^2}\right)U-\right.$$
$$\left.\frac{R_c\left(r+R_c\right)}{1-n_e}\frac{\partial P}{\partial x}\left(r+R_c\right)\right] \tag{34}$$

where linear operator and initial guess is defined as

$$L_U=\left(r+R_c\right)^2\frac{\partial^2}{\partial r^2}+\left(r+R_c\right)\frac{\partial}{\partial r}-1 \tag{35}$$

$$U_{10}=\frac{R_c\left(r+R_c\right)}{2(1-n_e)}\frac{\partial P_0}{\partial x}\left(r+R_c\right)\ln\left(r+R_c\right)+ C_7\left(r+R_c\right)+\frac{C_8}{r+R_c}. \tag{36}$$

The homotopy perturbation method suggests that we can write Eq. (34)as follow

$$H(Q,U)=(1-Q)\left\{L[U]-L[U_{10}]\right\}+\{QL[U]+ \frac{2w_e n_e}{1-n_e}[\left(r+R_c\right)^2(\frac{\partial U}{\partial r})(\frac{\partial^2 U}{\partial r^2})-\left(r+R_c\right) (\frac{\partial^2 U}{\partial r^2})U-\frac{R_c\left(r+R_c\right)}{1-n_e}\frac{\partial P}{\partial x}\left(r+R_c\right)]\}, \tag{37}$$

According to method procedure, we define as

$$U=U_0+QU_1+Q^2U_2+..., \qquad F=F_0+QF_1+Q^2F_2+..., \tag{38}$$

Where Q is the embedding parameter, substituting above Eq. (38) into Eq. (37) and take $Q\to 1,$ we arrive at

$$U=\frac{R_c\left(r+R_c\right)}{2(1-n_e)}\frac{dP}{dx}\left(r+R_c\right)\ln\left(r+R_c\right)+(C_7+C_9) \left(r+R_c\right)+\frac{(C_8+C_{10})}{r+R_c}+\frac{a_2 w_e}{8\left(r+R_c\right)^3}+ \frac{a_4}{2}\left(r+R_c\right)\ln\left(r+R_c\right). \tag{39}$$

Using Eq. (39) in Eq. (23), we get

$$\frac{dP}{dx}=\frac{F-C_{11}}{C_5}. \tag{40}$$

7. RESULTS AND DISCUSSION

To analyze the imperative aspect in this paper we have considered three different types of tapering effects on a curved arteries having mild stenosis by plotting the graphs of wall shear stress, wall shear stress at the throat of stenosis and impedance resistance to blood flow with the help of the different emerging flow parameters such as stenosis height, stenosis shape, curvature, Weissenberg number and shear thinning fluid parameter by keeping parameters constant as $F=0.09,$ $\sigma=0.01,$ $\delta=0.09,$ $n_e=0.1,$ $w_e=0.1,$ L=2, $R_c=3.1,$ $n=2$.

Figs. (2) to (6)are plotted to show the influence of stresses on the wall of curved arteries in the presence stenosis with axial distance *x*. It is observed from these figures that stresses on the wall of stenosed arteries start steeply decreasing towards the downstream of the stenotic segment and then start rapidly increasing towards the end of the stenotic segment. The wall shear stress for different values of fluid parameter n_e is given in Fig. (2). It is observed from this figure that stresses on the wall of curved arteries increases with an increase in shear thinning fluid parameter n_e. Fig. (3) is plotted for different values of Weissenberg number w_e which is the ratio of the relaxation time and a specific process time of fluid. It is observed from graph that by increasing Weissenberg number there will be increase in relaxation time and when we relax time flow can move easily, so stresses on the wall of curved arteries decreases. The wall shear stress for different values of stenosis height δ and curvature R_c are given in Figs. (4) and (5). It is observed that the stresses on the wall arteries are inversely related to the stenosis height and directly related to the curvature of the curved arteries. The effect of stenosis shape n with different tapering is given in Fig. (6). It is observed that a stress on the wall of the curved arteries increases between the region $0\le x\le 0.57$, while opposite trend is observed in the rest of region. The velocity profile for different tapering effectsis given in Figs. (8) and (9). It is observed from these graphs that the velocity profile increases at the center of the stenosed arteries with an increase in the values of stenosis height δ and Weissenberg number w_e between the interval $-0.46\le r\le 0.54,$ while opposite trend is observed near the wall of stenosed arteries between the interval $-0.88\le r\le -0.45$ and $0.55\le r\le 0.89.$ It is observed from these graphs that amplitude for converging tapering is higher at the center of the arteries as compared to the near of the wall of curved arteries. The distribution for wall shear stress at the stenosis throat against the maximum height of stenosis δ is plotted through Figs.(10)-(12). The wall shear stress at the stenosis throat for different values of shear thinning fluid parameter n_e and Weissenberg number w_e are given in Figs. (10) and (11). It is observed that shear stress at the throat of stenosis for curved arteries increases by increasing the values of shear thinning fluid parameter n_e, while opposite behavior at the throat of stenosis is observed for Weissenberg number w_e. Fig. (12) is plotted for shear stress at throat of stenosis for different values of curvature R_c and observed stresses at throat of stenosis decreases with an increase in the curvature of the curved arteries. The resistance impedance to blood flow along maximum height of stenosis δ for different type of stenosed arteries are plotted from Figs. (13)-(16) and observed in these figures that impedance resistance to blood flow is maximum near the peak of stenosis, which gives higher amplitude for

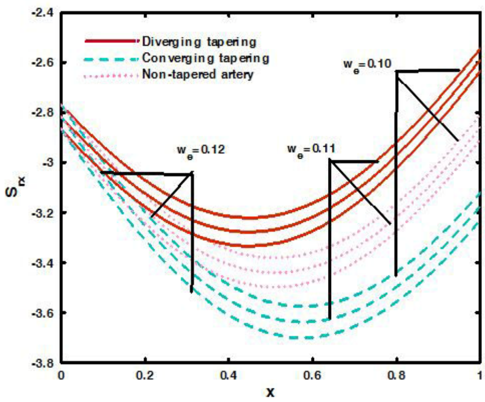

Figs. 2. Variation of wall shear stress for $n_e = 0.1,$

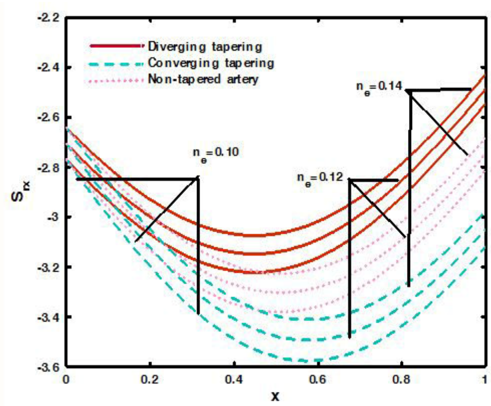

Figs. 3. Variation of wall shear stress for $w_e = 0.1.$

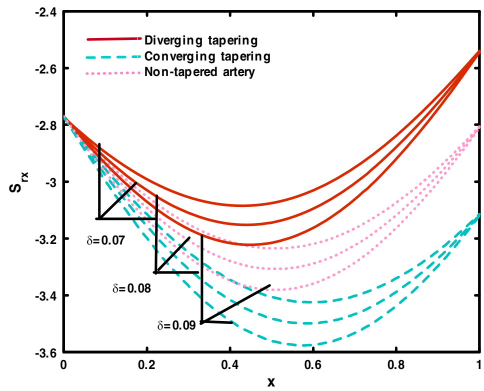

Figs. 4. Variation of wall shear stress for $R_c = 3.1,$

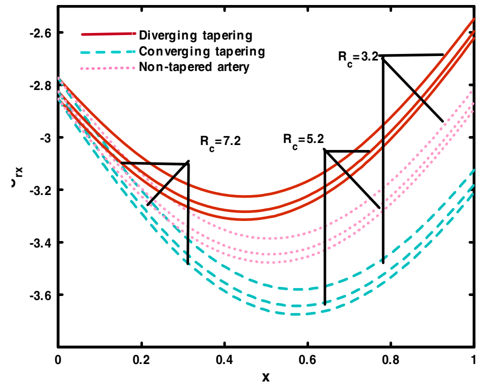

Figs. 5. Variation of wall shear stress for $\delta = 0.09.$

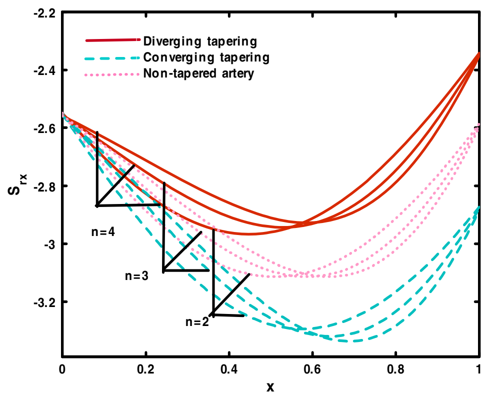

Figs. 6. Variation of wall shear stress for stenosis shape $n,$

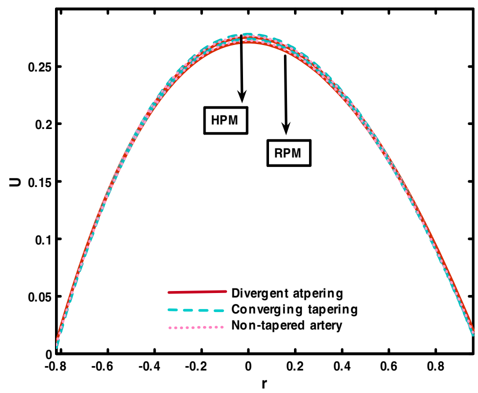

Figs. 7. Comparison of velocity profile between RPM and HPM.

converging tapering as compare to other associated tapering. The effect of stenosis shape n and curvature R_c on resistance impedance to flow is given in Figs. (13) and (14). It is analyzed that impedance resistance to blood flow decreases by increasing the values of the stenosis shape and curvature of the curved arteries. It is important to note here the resistance to blood flow is maximum for the symmetric stenosis case$n$=2. The effect of the Weissenberg number w_e on resistance impedance to flow is given in Figs. (15). It is observed that resistance impedance to flow increases with an increase in maximum height of stenosis and decreases with an increase in the Weissenberg number w_e. Fig. (16) is plotted for shear thinning fluid parameter n_e and observed that the resistance impedance to blood flow decreases when the fluid is thinner then thicker. Trapping phenomenon has been discussed to show the blood flow pattern in the curved arteries through Figs. (17)-(19). It is observed here that the trapping is now not symmetric about the central line of the

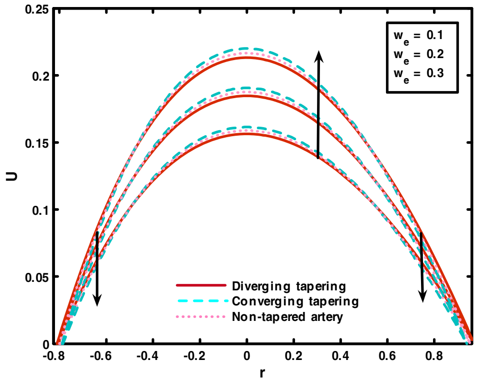

Figs. 8. Variation of velocity profile for $\delta = 0.09,$

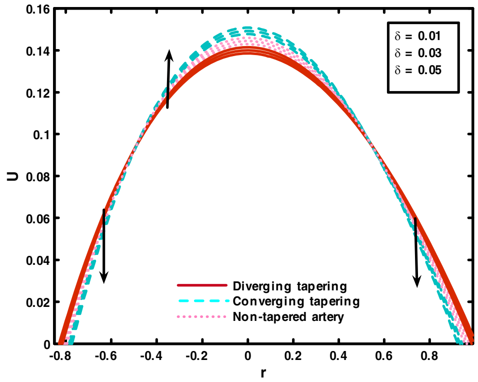

Figs. 9. Variation of velocity profile for $w_e = 0.1.$

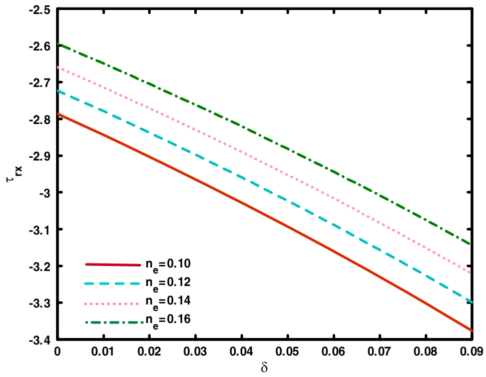

Figs. 10. Variation of wall shear stress at the throat of stenosis for $w_e = 0.1,$

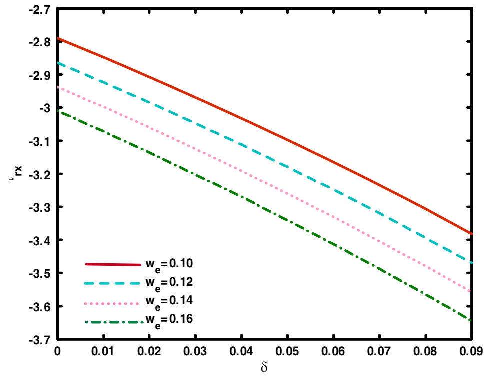

Figs. 11. Variation of wall shear stress at the throat of stenosis for $n_e = 0.1.$

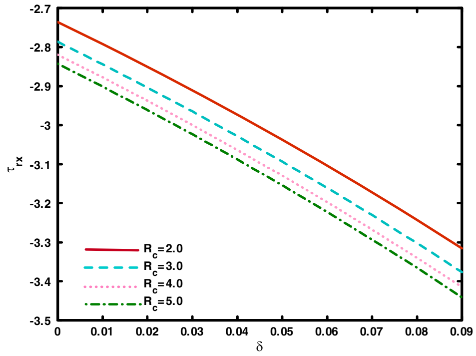

Fig. 12. Variation of wall shear stress at the throat of stenosis for R_c **.**

curved channel which is different from the case of straight or vertical channels. From Fig. (17) and it is depicted that the number of trapping bolus increases by increasing value of Weissenberg number w_e and shear thinning fluid parameter n_e. Fig. (19), shows that the symmetry of trapped bolus destroys due to increase in curvature of the curved arteries and cause to slight increase in the size of trapped bolus.Table(1) and Fig. (7) are plotted to show the comparison between two analytical techniques that both is effective and convenient to solve highly nonlinear equations. The main differences between both analytical techniques are that regular perturbation requires small parameters in the equations, while the homotopy perturbation is independent of small or large parameter.HPM method has significant advantage that is providing an approximate solution to a wide range of nonlinear problems in applied sciences. It has been observed from figure that these analytical techniques are quite close in this problem with some absolute error to solve nonlinear equations. Precision of the considered techniques increases if more components are elaborate in the series.

8. CONCLUSION

In this present analysis we have discussed the mathematical model of blood flow that has not done before from author's knowledge in the curved artery (or curved channel) with different tapering arteries. The basic objectives of the problem are to discuss wall shear stress and resistance impedance to flow to measure the reduction in blood flow in curved artery. The study involves the main points that are given as follows

- The solution of the resulting equation obtained by RPM and HPM are compared and at the end it is found that both the solution is almost equivalent with some absolute error.
- The combined effect of curvature and stenosis shows that stenosis dominant over the curvature of curved artery.
- The trapping phenomenon shows that the symmetry destroys due to increase in curvature R_c of curved arteries that pushed bolus away from the center of the channel.

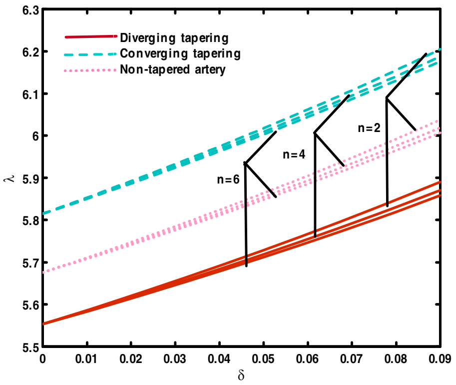

Figs. 13. Variation of resistance impedance for $R_c = 3.1,$

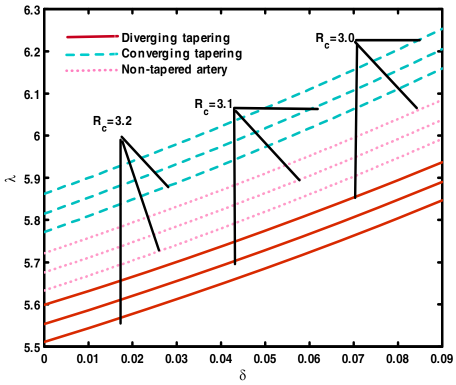

Figs. 14. Variation of resistance impedance for $n = 2.$

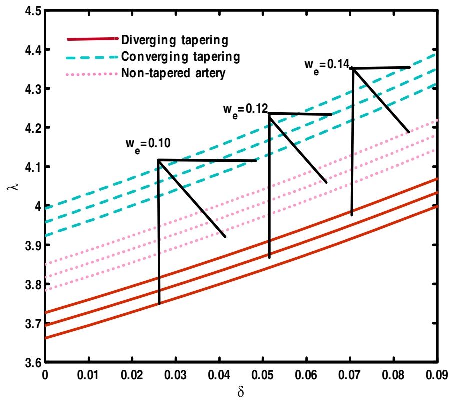

Figs. 15. Variation of resistance impedance for $n_e = 0.1,$

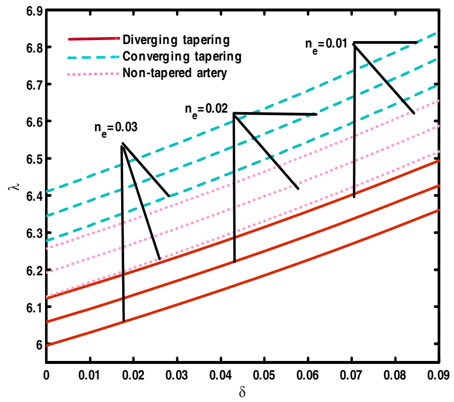

Figs. 16. Variation of resistance impedance for $w_e = 0.1.$

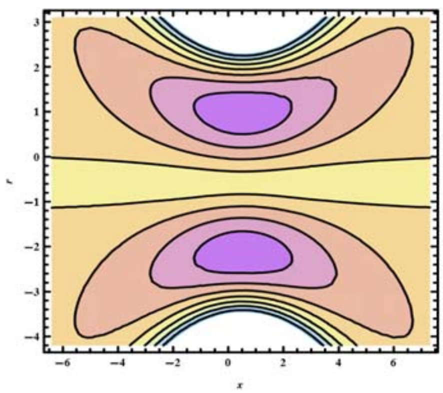

Fig. 17. Blood flow pattern for $w_e = 0.01,$

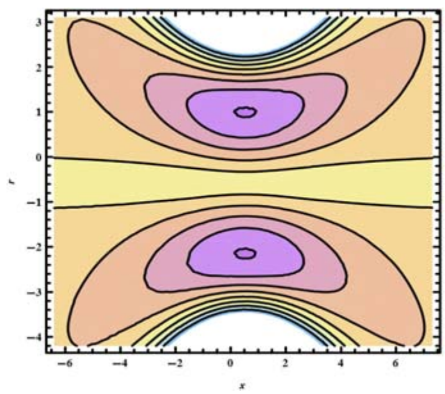

Fig. 18. Blood flow pattern for $w_e = 0.02.$

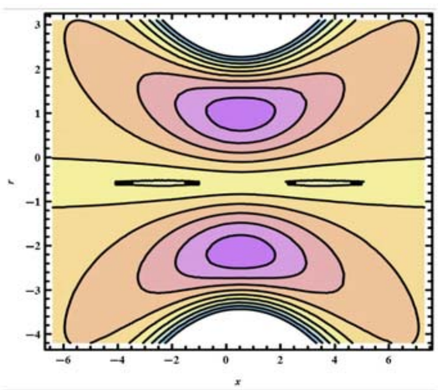

Fig. 18. Blood flow pattern for (a) $n_e = 0.01,$

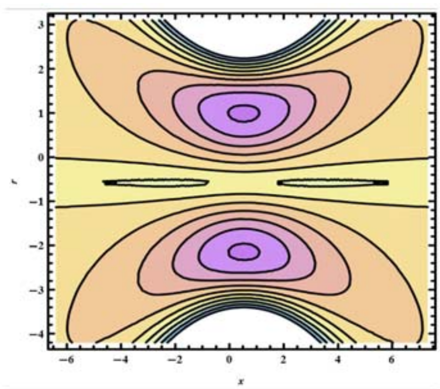

Fig. 18. Blood flow pattern for $n_e = 0.09.$

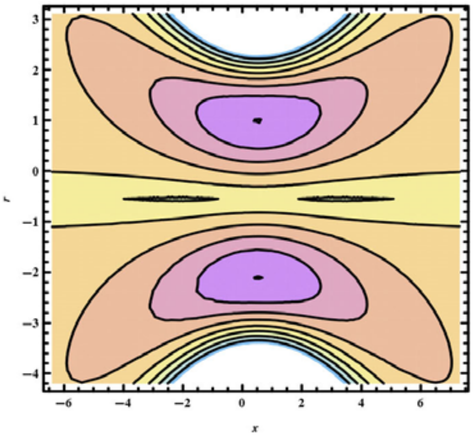

Fig. 19. Blood flow pattern for $R_c = 0.68$,

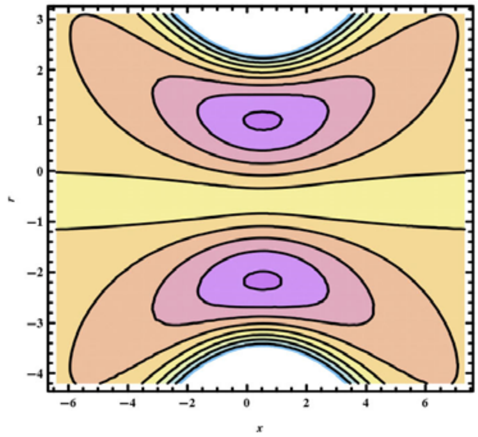

Fig. 20. Blood flow pattern for $R_c = 0.70$.

Table 1 Comparison for velocity profile between RPM and HPM

w	Diverging tapering			Converging tapering			Non tapered arteries		
r	HPM	RPM	$\|Error\|$	HPM	RPM	$\|Error\|$	HPM	RPM	$\|Error\|$
h	0.0000	0.0000	0.0000	0.0000	0.0000	0.0000	0.0000	0.0000	0.0000
0.8	0.0941	0.0932	0.0009	0.0916	0.0907	0.0009	0.0928	0.0919	0.0009
0.6	0.1699	0.1683	0.0016	0.1697	0.1679	0.0018	0.1698	0.1681	0.0017
0.4	0.2268	0.2245	0.0023	0.2281	0.2258	0.0023	0.2274	0.2252	0.0022
0.2	0.2626	0.2601	0.0025	0.2650	0.2623	0.0027	0.2638	0.2612	0.0026
0.0	0.2752	0.2724	0.0028	0.2779	0.2753	0.0026	0.2765	0.2738	0.0027
-0.2	0.2616	0.2589	0.0027	0.2639	0.2613	0.0026	0.2627	0.2601	0.0026
-0.4	0.2184	0.2162	0.0020	0.2194	0.2173	0.0021	0.2189	0.2167	0.0022
-0.6	0.1411	0.1398	0.0013	0.1401	0.1389	0.0012	0.1406	0.1392	0.0014
-0.8	0.0244	0.0242	0.0002	0.0200	0.0199	0.0001	0.0222	0.0220	0.0002
$-h$	-0.1391	-0.1376	0.0015	-0.1480	-0.1464	0.0016	-0.1436	-0.1419	0.0017

- The wall shear stress gives higher amplitude for diverging tapering, while resistance impedance to flow gives higher amplitude for converging tapering.
- The wall shear stress and shear stress at the throat of stenosis possess same behavior along maximum height of stenosis with respect to curvature R_c, Weissenberg number w_e and shear thinning fluid parameter n_e.
- The wall shear stress shows inverse and resistance impedance to blood flow shows direct relation with stenosis height δ.

REFERENCES

Canic, E. and H. K. (2003). Mathematical analysis of the quasilinear effects in a hyperbolic model blood flow through compliant axis-symmetric vessels. *Mathematical Methods in the Applied Sciences*26, 1161-1186.

Chakraborty, U. S., D. Biswas and M. Paul (2011). Suspension model blood flow through an inclined tube with an axially non-symmetrical stenosis. *Korea Australia Rheology Journal*23, 25-32.

Ellahi, R., S. U. Rahman, M. Gulzar, S. Nadeem and K. Vafai (2014). A mathematical study of non-Newtonian micropolar fluid in arterial blood flow through composite stenosis. *Applied Mathematics and Information Sciences*4, 1567-1573.

Hasan, A. B. M. T. and D. K.Das (2008). Numerical simulation of sinusoidal fluctuated pulsatile laminar flow through stenoticartery. *Journal of*

Applied Fluid Mechanics 1, 25-35.

J. H. (2005). Application of homotopyperturbation method to nonlinear wave equations. *Chaos, Solitons and Fractals*26, 695-700.

Jung, H., J. W. Choi and C. G. Park (2004). Asymmetric flows of non-Newtonian fluids in symmetric stenosed artery. *Korea-Australia Rheology Journal*16, 101-108.

Liu, G. T., X. J. Wang, B. Q. Ai and L. G. Liu (2004). Numerical study of pulsatile flow through a tapered artery with stenosis. *Chinese Journal of Physics* 42, 401-409.

Mandal, D. K., N. K. Manna and S. Chakrabarti (2011). Influence of primary stenosis on secondary one and vice versa in case of double stenoses. *Journal of Applied Fluid Mechanics*4, 31-42.

Mekheimer, K. S. and M. A. ElKot (2008). The micropolarfluid model for blood flow through a tapered artery with a stenosis. *Acta Mechanica Sinica* 24, 637-644.

Nadeem, S. and E. N. Maraj (2013). The MathematicalAnalysis for Peristaltic Flow of Hyperbolic Tangent Fluid in a Curved Channel. *Communications in Theoretical Physics* 59, 729-736.

Nadeem, S. and S. Akram (2009). Peristaltic transport of a Hyperbolic Tangent Fluid Model in an Asymmetric Channel. *Zeitschriftfür Natur forschung A*64a, 559-567.

Nadeem, S. and S. Ijaz (2015). Mechanics of biologicalblood flow analysis through curved artery with stenosis, *Journal of Mechanics in Medicine and Biology*.

Nadeem, S., N. S. Akbar and H. Sadaf (2015). Effects ofnanoparticles on the peristaltic motion of tangent hyperbolic fluid model in an annulus, *Alexandria Engineering Journal*, 54, 843–851.

Nadeem, S., N. S.Akbar and M.Ali (2012). Influence ofheat and chemical reactions on hyperbolic tangent fluid model for blood flow through a tapered artery with a stenosis, *Heat Transfer Research* 43, 69-94.

Reddy, J. V., D. Srikanth and S. K.Murthy (2014). Mathematical modeling of couple stress on fluid flow in constricted tapered artery in the presence of slip-effects of catheter. *Applied Mathematics and Mechanics* 35, 947-958.

Sankar, D. S. and K. Hemalatha (2007). A non-Newtonian fluid flow model for blood flow through a catherized artery. *Applied Mathematical Modelling*31, 1847-1864.

Sankar, D. S. and L. Usik (2009). Mathematical modellingof pulsatile flow of non-Newtonian fluid in stenosed arteries. *Communications in Nonlinear Science and Numerical Simulation* 14, 2971-2981.

Young, D. F. and F. Y. Tsai (1973). Flow characteristics in model of arterial stenosis steady flow. *Journal of Biomechanics* 6, 395-410.

APPENDIX

$$C_1 = -(-\frac{dP_0}{dX}R_c^3 - \frac{dP_0}{dX}R_c^3\ln R_c - h^2\frac{dP_0}{dX}R_c\ln(h+R_c) - 2h\frac{dP_0}{dX}R_c^2\ln(h+R_c) - \frac{dP_0}{dX}R_c^3\ln(h+R_c))/(2(n_e-1)(h^2+2hR_c+2R_c^2)),$$

$$C_2 = -(h^2\frac{dP_0}{dX}R_c^3 + 2h\frac{dP_0}{dX}R_c^4 + \frac{dP_0}{dX}R_c^5 + h^2\frac{dP_0}{dX}R_c^3\ln R_c + \frac{dP_0}{dX}R_c^5\ln R_c - h^2\frac{dP_0}{dX}R_c^3\ln(h+R_c) - 2h\frac{dP_0}{dX}R_c^4\ln(h+R_c) + R_c) + 2h\frac{dP_0}{dX}R_c^4\ln R_c + \frac{dP_0}{dX}R_c^5\ln(h+R_c))/(2(n_e-1)(h^2+2hR_c+2R_c^2)),$$

$$C_3 = (4R_c^4(h+R_c)^2(a_3 - a_3n_e + (a_3 - a_3n_e + \frac{dP_1}{dX}R_c) + a_2(-1+n_e)(3h^2+6hR_c+2R_c^2) + 4R_c^2(h+R_c)^2(a_3 - a_3n_e + \frac{dP_1}{dX}R_c)(R_c^2\ln R_c + (h+R_c)^2\ln(h+R_c)))/(8(-1+n_e)R_c^2(h+R_c)^2(h^2+2hR_c+2R_c^2)),$$

$$C_4 = -(4R_c^4(h+R_c)^4(a_3 - a_3n_e + \frac{dP_1}{dX}R_c) + a_2(-1+n_e)(3h^4+12h^3R_c+18h^2R_c^2+12R_c^3+4R_c^4) + 4R_c(h+R_c)^4(a_3 - a_3n_e + h\frac{dP_1}{dX}R_c)(\ln R_c - \ln(h+R_c)))/(8(-1+n_e)R_c^2(h+R_c)^2(h^2+2hR_c+2R_c^2)),$$

$$C_5 = (R_c(h(h+R_c)(h^2+2hR_c+2R_c^2) + 4R_c^2(h+R_c)^2(\ln R_c - \ln(h+R_c))(2+\ln R_c - \ln(h+R_c))))/(8(-1+n_e)(h^2+2hR_c+2R_c^2)),$$

$$C_6 = -(n_e(\frac{dP_0}{dX})^2R_c^2(h(h+R_c)(h^6+6h^5R_c+28h^4R_c^2+72h^3R_c^3+100h^2R_c^4+72hR_c^5+24R_c^6) + 4R_c^2(h+R_c)^2(3h^4+12h^3R_c+18h^2R_c^2+12hR_c^3+4R_c^4)(\ln R_c - \ln(h+R_c))(3+3\ln R_c+(\ln R_c)^2-(3+2\ln R_c)\ln(h+R_c)(\ln(h+R_c))^2)))/(16(-1+n_e)^3(h^2+2hR_c+2R_c^2)^3),$$

$$a_1 = 2n_e/(1-n_e),\ a_2 = 16C_2^2a_1/4, C_7 = C_1, C_8 = C_2,\ a_3 = -((\frac{dP_0}{dX})^2R_c^2a_1)/(4(-1+n_e)^2), a_4 = (\frac{dP_0}{dX}R_c)/(n_e-1) + a_3w_e,$$

$$C_9 = (4R_1^4(h+R_c)^2(a_4 - a_4n_e + \frac{dP_1}{dX}R_c) + a_2(-1+n_e)(3h^2+6hR_c+2R_c^2)w_e + 4R_1^2(h+R_c)^2(a_4 - a_4n_e + \frac{dP_1}{dX}R_c)(R_c^2\ln R_c + (h+R_c)^2\ln(h+R_c)))/(8(-1+n_e)R_c^2(h+R_c)^2(h^2+2hR_c+2R_c^2)),$$

$$C_{10} = -(4R_c^4(h+R_c)^4(a_4 - a_4 n_e + \frac{dP_1}{dX}R_c) + a_2(-1+n)(3h^4 + 12h^3R_c + 18h^2R_c^2 + 12hR_c^3 + 4R_c^4)w_e + 4R_c^4(h+R_c)^4(a_4 - a_4 n_e + \frac{dP_1}{dX}R_c)(\ln R_c - \ln(h+R_c)))/(8(-1+n_e)R_c^2(h+R_c)^2 (h^2 + 2hR_c + 2R_c^2)),$$

$$C_{11} = -(\frac{dP_0}{dX}R_c(h(h+R_c)(2(-1+n_e)^2(h^2+2hR_c+2R_c^2)^2(h^2 + 2hR_c + 4R_c^2) + n_e\frac{dP_0}{dX}R_c(h^6 + 6h^5R_c + 28h^4R_c^2 + 72h^3 R_c^5 + 100h^2R_c^4 + 72hR_c^5 + 24R_c^6)w_e) + 4R_c^2(h+R_c)^2(4 (-1+n_e)^2(h^2+2hR_c+2R_c^2)^2 + 3n_e\frac{dP_0}{dX}R_c(3h^4 + 12 h^3R_c + 18h^2R_c^2 + 12hR_c^3 + 4R_c^4)w_e + (2n_e(-1+n_e)^2(h^2 + 2hR_c + 2R_c^2)^2 + 3n_e\frac{dP_0}{dX}R_c(3h^4 + 12h^3R_c + 18h^2R_c^2 + 12hR_c^3 + 4R_c^4)w_e) + n_e\frac{dP_0}{dX}R_c(3h^4 + 12h^3R_c + 18h^2R_c^2 + 12hR_c^3 + 4R_c^4)w_e(\ln R_c - \ln(h+R_c)))(\ln R_c - \ln(h+R_c))) (\ln R_c - \ln(h+R_c))))/(16(-1+n_e)^3(h^2+2hR_c+2R_c^2)^3).$$